

# Preparation of ZnO-SnO<sub>2</sub> ceramic materials by a coprecipitation method

M. PEITEADO\*,<sup>1</sup> Y. IGLESIAS,<sup>2</sup> J. DE FRUTOS,<sup>3</sup> J. F. FERNÁNDEZ,<sup>2</sup> A. C. CABALLERO<sup>2</sup>

<sup>1</sup> Advanced Materials Department, Jozef Stefan Institute, 1000 Ljubljana, Slovenia.

<sup>2</sup> Departamento de Electrocerámica, Instituto de Cerámica y Vidrio (CSIC), 28049 Madrid, España.

<sup>3</sup> Departamento de Física Aplicada, ETSI Telecomunicaciones (UPM), 28040 Madrid, España.

Tin (IV)-doped zinc oxide ceramics find its main application as specific gas sensor devices. The sensor ability of the mixture and its particular affinity for a particular gas (selectivity) depends both on the crystalline phases in the microstructure of the sintered semiconductor and on the degree of tin incorporation into ZnO lattice. By means of a highly reactive coprecipitation method it is revealed that the range of solid solution of tin in zinc oxide stays below 0.1 mol % of SnO<sub>2</sub> since higher concentrations lead to segregation of a secondary Zn<sub>2</sub>SnO<sub>4</sub> spinel type-phase.

*Keywords:* doping, microstructure, semiconductor, ZnO.

## Obtención de materiales cerámicos basados en ZnO-SnO<sub>2</sub> por coprecipitación.

Los materiales cerámicos basados en óxido de cinc dopado con estaño (IV) encuentran su principal aplicación como dispositivos sensores específicos de gases. La capacidad sensora de la mezcla de óxidos y su particular afinidad por un determinado gas específico (selectividad) es función directa de cuáles sean las fases cristalinas presentes en la microestructura del semiconductor sinterizado, así como del grado de incorporación del estaño en la red del ZnO. La obtención del polvo cerámico de partida por un método de coprecipitación altamente reactivo revela que el rango de solución sólida del estaño en el óxido de cinc se encuentra por debajo del 0.1 % en moles de SnO<sub>2</sub>; concentraciones superiores llevan a la segregación de una fase secundaria, Zn<sub>2</sub>SnO<sub>4</sub> con estructura de tipo espinela.

*Palabras clave:* dopante, microestructura, semiconductor, ZnO.

## 1. INTRODUCTION

Materials containing polycrystalline zinc stannates, both in the form of bulk and thin film devices, show potential applications in the field of gas sensors, electrodes for solar batteries, detectors of moisture and transparent electronics (1-3). Actually the name zinc stannate describes to different oxides with different crystallographic structures and zinc-to-tin ratios: the Zn<sub>2</sub>SnO<sub>4</sub> orthostannate of zinc formed in the cubic spinel crystal structure and the orthorhombic ZnSnO<sub>3</sub> metastannate. However data on the existence of this last one are still ambiguous and contradictory and more detailed studies on the structure are still needed. For example Sheng and Zhang obtained a pure ZnSnO<sub>3</sub> phase with a perovskite-type structure by using a co-precipitation method with oxalic acid and ammonia as precipitants (4). Looking into the ionic radius of Zn<sup>2+</sup>, Kovacheva et al. however stated that ZnSnO<sub>3</sub> cannot adopt a perovskite structure under normal conditions, and by means of a low-temperature ion exchange technique (using Li<sub>2</sub>SnO<sub>3</sub> and ZnCl<sub>2</sub>) they prepared ZnSnO<sub>3</sub> with an ilmenite-type structure (5). Any other attempt to prepare pure ZnSnO<sub>3</sub> by different methods has failed but in any case, if crystalline ZnSnO<sub>3</sub> exists, it should be exhibiting a limited thermal stability as the only stable phases at high temperatures in the ZnO-SnO<sub>2</sub> system seem to be Zn<sub>2</sub>SnO<sub>4</sub>, ZnO and SnO<sub>2</sub> (6).

But besides the discrepancies on the thermal evolution of ZnO-SnO<sub>2</sub> binary system, few efforts have been devoted on the possibility of incorporate tin (IV) on zinc oxide lattice. The fact is that very little is known about the behaviour of Sn in zinc

oxide, most of the knowledge coming from the field of ZnO-based varistors (7-9). Zinc oxide with a wurtzite structure is naturally a direct wide band gap n-type semiconductor which nevertheless requires the presence of donor impurities to improve its electrical conductivity (10,11). Different elements of group III and other Zn-substituting elements has yielded a low resistivity n-type ZnO, but more recently special attention has been paid to the ZnO-SnO<sub>2</sub> system; it is expected that this dopant will act as double ionized donor impurity in ZnO lattice so contributing to increase the semiconductor behaviour of this oxide (12). As mentioned such property will find a wide utility in different electroceramic applications (2,9,13,14) and more recently represents a great challenge in the field of room temperature ferromagnetic devices (15-17).

Within this framework the present contribution is mainly focused on tin doped-ZnO materials prepared by a highly reactive co-precipitation route in order to clarify the microstructural evolution of the binary system as well as to determine the grade of incorporation of tin (IV) into the zinc oxide lattice.

## 2. EXPERIMENTAL

The study was carried out over three ZnO-based compositions doped with different amounts of tin oxide: 0.1, 1 and 10 mol % of SnO<sub>2</sub>. The materials were prepared by co-precipitating Zn<sup>2+</sup> y Sn<sup>4+</sup>, using respectively

Zn(CH<sub>3</sub>COO)<sub>2</sub>·2H<sub>2</sub>O and SnCl<sub>4</sub>·5H<sub>2</sub>O as precursors and NaOH as precipitant agent. In all cases raw materials of above 99.99% of purity were used (Sigma-Aldrich). Both precursors were first dissolved in deionized water to form two transparent solutions and then mixed together. Concentrated NaOH (1M) was added dropwise to the vigorously stirred mixed solution and the final pH value was adjusted to about 10 to promote a complete precipitation of both cations. The resulting slurry was filtered, washed with butylamine to remove the counteranions (chlorides mainly) and dried at 85°C for 24 hours. The dried powder was finally calcined at 450°C for 4 hours to obtain the oxides. To obtain dense pellets, samples of each composition were uniaxially pressed at 120 MPa into discs of 0.3 cm height × 2 cm diameter and then sintered in air at 1300°C for 2h.

Evolution of crystalline phases in the ZnO-SnO<sub>2</sub> system was followed by X-Ray Diffraction of powder samples treated at different calcination temperatures and 1 hour soaking time, in a D-5000 Siemens Diffractometer (Cu Kα1 radiation). Shape, size and composition of these powders were observed on a Transmission Electron Microscope (TEM, Model 7100 Hitachi) supplied with an Energy Dispersed Spectroscopy microanalysis probe (EDS). The sintered specimens were also characterized by means of Scanning Electron Microscopy on a Cold Field Emission-Scanning Electron Microscope (FE-SEM Model S-4700 Hitachi) over polished and chemically etched surfaces. Grain size measurements were evaluated from FE-SEM micrographs by an image processing and analysis program that measures the surface of each ZnO grain and transforms its irregularly shaped area into a circle of equivalent diameter; more than 400 grains were considered for each measurement.

### 3. RESULTS AND DISCUSSION

Thermal evolution of crystalline phases for the system with 10 mol % of SnO<sub>2</sub> is illustrated in XRD spectra of Figure 1, and a similar behaviour was obtained for the other two compositions with lower amounts of dopant (not depicted here). As observed, above 1000°C the system is composed by a mixture of two phases, the major ZnO and a spinel type phase corresponding to Zn<sub>2</sub>SnO<sub>4</sub>. At lower temperatures an intermediate compound is formed, which gradually transforms into the spinel phase as the temperature is increased. JCPDS files (Joint Committee on Powder Diffraction

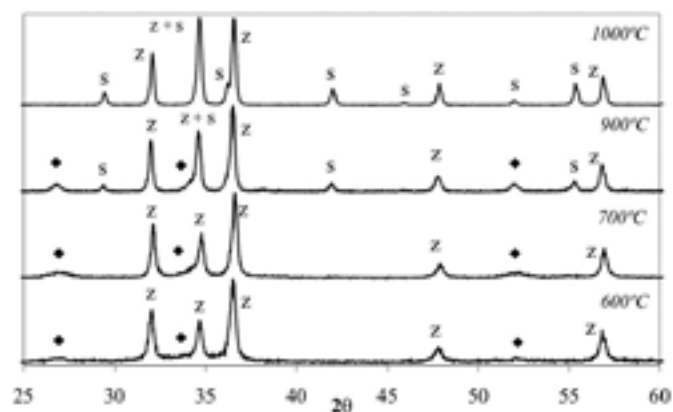


Fig. 1- XRD patterns of sample with 10 mol % SnO<sub>2</sub> at different calcination temperatures. Z: ZnO, S: Zn<sub>2</sub>SnO<sub>4</sub> spinel-type phase, ® Black rhombus indicate those peaks belonging either to SnO<sub>2</sub> or ZnSnO<sub>3</sub> phases.

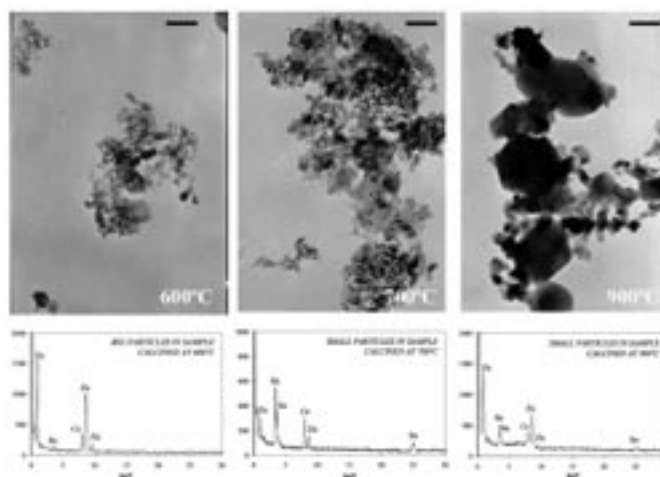


Fig. 2- TEM micrographs and EDS analyses of composition with 10 mol % of SnO<sub>2</sub> at different temperatures. (Scale bar = 50 nm).

Standards) indicate that this intermediate phase could be associated either with tetragonal SnO<sub>2</sub> cassiterite (JCPDS file n° 41-1445) or with ZnSnO<sub>3</sub> compound (JCPDS file n° 28-1486). In fact some authors have attributed these signals to a two phase mixture of Zn<sub>2</sub>SnO<sub>4</sub> and SnO<sub>2</sub> (5), whereas other authors ascribed it to single ZnSnO<sub>3</sub> phase (4). In an attempt to clarify this feature TEM micrographs of powders calcined between 600 and 900°C were performed. Again a similar behaviour was obtained for the three compositions but the stronger differences were observed for the system with the higher amount of dopant (10 mol %) whose micrographs are depicted in Figure 2. As can be seen at 600°C it is found the existence of big hexagonal-shaped units of 30-40 nm in size, together with small rounded particles of approximately 10-5 nm. Although semi-quantitative, EDS analysis corresponding to this sample indicates that bigger particles are zinc-rich while the smaller ones are mainly composed by tin; this allows its identification with respectively ZnO and SnO<sub>2</sub>. None of the analyses performed at this temperature however indicated the presence of the ZnSnO<sub>3</sub> phase. Increasing the temperature leads to a higher size of these two groups of particles but they still preserve the same chemical composition without any trace of ZnSnO<sub>3</sub>. Finally at 900°C the observed microstructure encloses big grains of ZnO and other particles which are now visibly larger than in previous calcinations. Once more EDS analyses allowed the identification of ZnO particles together with a second phase which can now be associated with the Zn<sub>2</sub>SnO<sub>4</sub> spinel-type phase attending to the obtained Zn:Sn ratio (equal to 2:1, Figure 2). It should be stated however that although XRD data indicated the presence of three different phases at 900°C, it was not possible to clearly distinguish them in TEM images probably because it is a highly reactive system in which different reactions between the involved phases are taking place at this temperature. Nevertheless, again no evidence of ZnSnO<sub>3</sub> was ever detected, suggesting that this phase is rather quite unstable in this system and can not be stabilized with this co-precipitation method.

With regard to the range of solid solution of tin in zinc oxide, Figure 3 now illustrates the results of XRD analyses for samples of the three compositions sintered at 1300°C and 2h. Again the XRD spectrum of sample with 10 mol % of tin, and also that of composition with 1 mol % of dopant, evidence a

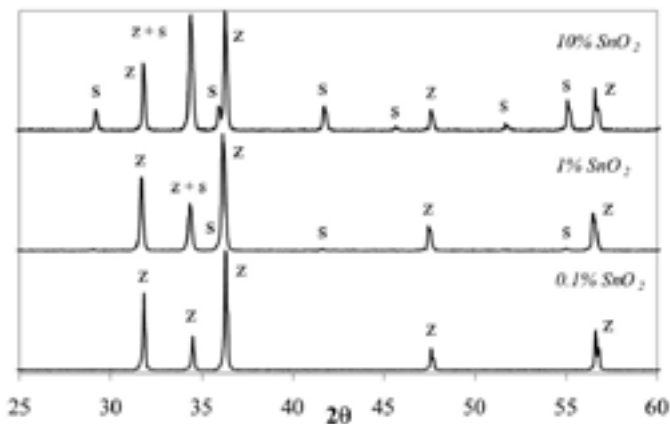


Fig. 3- XRD patterns of samples of the three compositions sintered at 1300°C for 2 hours. Z: ZnO, S:  $Zn_2SnO_4$  spinel phase.

two-phase system composed by ZnO and the  $Zn_2SnO_4$  spinel phase. In the composition with lower amount of  $SnO_2$  no peaks of the spinel phase are however detected but this should be better attributed to its low concentration with regard to ZnO, clearly under the detection limit of the technique. Nevertheless SEM images of the three sintered compositions shown in Figure 4 undoubtedly indicate a biphasic system even for composition with just 1 mol % of tin oxide. At these low doping levels the general microstructure is dominated by large ZnO grains as in pure undoped ZnO, but small spherical particles of a secondary phase are now observed at triple points and along ZnO grain boundaries. EDS analyses depicted in Figure 5 confirm the presence of both zinc and tin in these particles with a composition near to the  $Zn_2SnO_4$  spinel-type compound (66% ZnO and 33%  $SnO_2$ ). Furthermore twin boundaries are also developed in almost each ZnO grain, which in addition to the pinning effect of the spinel particles lead to a gradual decrease in the average size of ZnO grains (9,18,19). As observed in the micrographs such a decrease becomes drastic for higher concentrations of  $SnO_2$  since it promotes a rapid increase in the volume fraction of the spinel phase, even though the average size of spinel grains scarcely changes (see also data in Table 1).

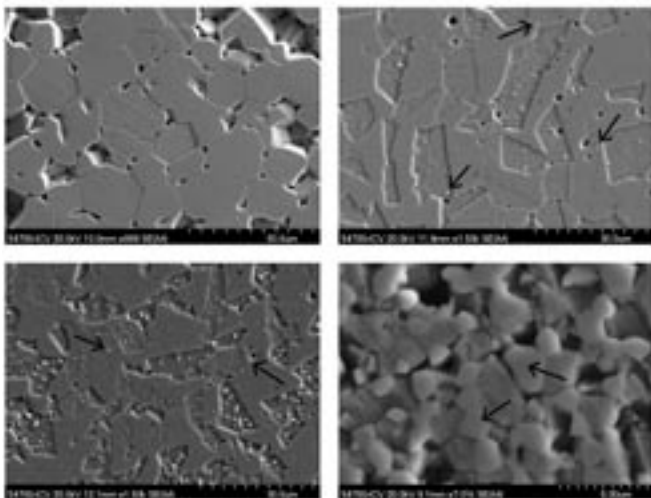


Fig. 4- Left to right and up to down, SEM micrographs of pure undoped ZnO and 0.1, 1 and 10 mol %  $SnO_2$ -doped compositions (samples sintered at 1300°C for 2 hours). Black arrows point to particles (grains) of secondary phase.

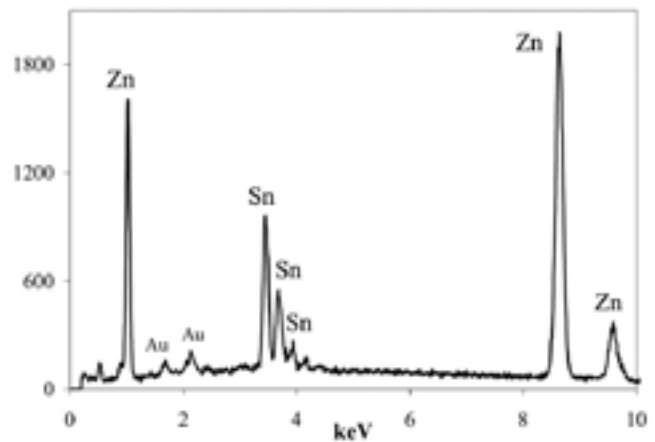


Fig. 5- EDS analysis of grains of secondary phase in samples sintered at 1300°C/2h. The obtained spectrum fits the proportions of  $Zn_2SnO_4$  compound (66% ZnO and 33%  $SnO_2$ ).

TABLE I. EVOLUTION OF ZnO GRAIN SIZE AND SPINEL GRAIN SIZE AS A FUNCTION OF DOPANT CONCENTRATION FOR SAMPLES SINTERED AT 1300°C/2H. THEORETICAL VALUES OF VOLUME FRACTION OF THE SPINEL PHASE CORRESPOND TO THE CASE IN WHICH ALL THE ADDED  $SnO_2$  WOULD FULLY INCORPORATE INTO  $Zn_2SnO_4$  SPINEL STRUCTURE.

	$G_{ZnO}$ ( $\pm 0.5\mu m$ )	$G_{spinel}$ ( $\pm 0.5\mu m$ )	% vol. spinel phase (theoretical)	% vol. spinel phase (experimental)
Undoped ZnO	17.4	-	-	-
+ 0.1 % mol $SnO_2$	12.9	0.9	0.3 %	0.3 %
+ 1 % mol $SnO_2$	7.6	0.9	3.3 %	3.3 %
+ 10 % mol $SnO_2$	1.8	1.0	32.5 %	32.4 %

But data in Table 1 also show that practically all the tin oxide should be forming part of the spinel structure, since the experimental values of the spinel volume fraction coincide with the theoretical values for a complete incorporation of  $SnO_2$  into  $Zn_2SnO_4$  phase. This is observed even in the case of composition with 0.1 mol % of  $SnO_2$ . However EDS analyses of samples sintered at 1300°C/2h indicate that a certain amount of tin could also be found inside ZnO grains. This is inferred both from the mapping of zinc and tin concentrations showed in Figure 6, which corresponds to sample with 10 mol % of  $SnO_2$ , as well as from the presence of a slight but sharp signal of tin inside the ZnO grains of this same sample. Therefore the solid solution of tin into ZnO lattice should not be completely excluded and its range should be found to be under 0.1 mol % of  $SnO_2$ .

#### 4. CONCLUSIONS

Tin doped zinc oxide-based materials have been prepared by a highly reactive co-precipitation method. Characterization of dense samples reveals that the range of solid solution of tin into ZnO lattice stays below 0.1 mol % of  $SnO_2$ . Higher concentrations give place to phase segregation and the formed biphasic system is composed by ZnO and a secondary  $Zn_2SnO_4$  spinel-type phase which restrains ZnO grain growth.

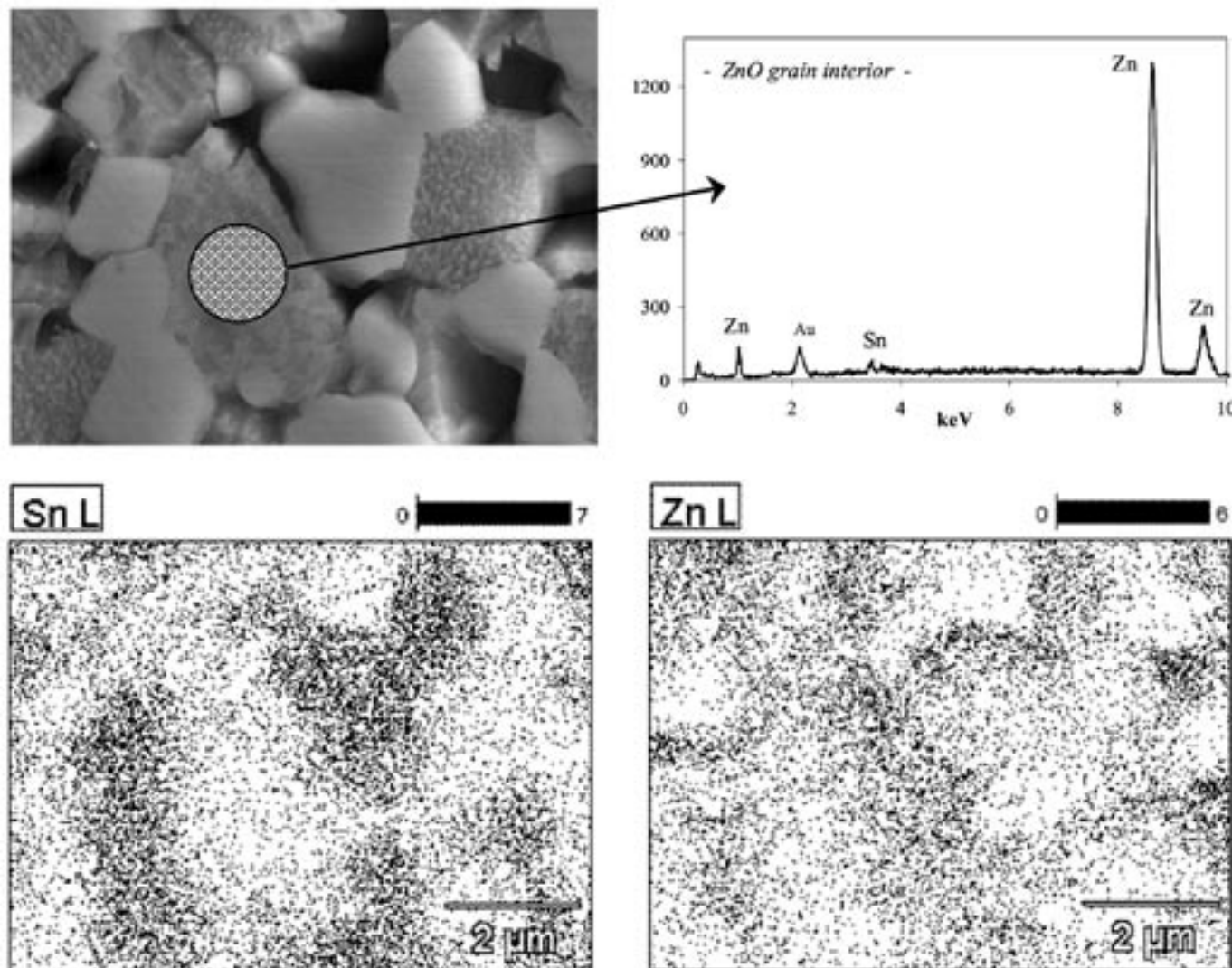


Fig. 6- Mapping of tin and zinc concentrations in sample with 10 mol % of SnO<sub>2</sub> sintered at 1300°C/2h. On the right upper corner EDS analysis confirming the presence of tin inside ZnO grains.

This spinel phase is gradually formed from the reaction between ZnO and SnO<sub>2</sub> and no trace of ZnSnO<sub>3</sub> compound is ever detected.

#### ACKNOWLEDGEMENTS

This work has been conducted within the CICYT MAT 2004-04843-C02-01 project. The authors would like to express its gratitude to the company INAEL S.A. (Toledo, Spain). Dr. Peiteado also acknowledges the Secretaría de Estado de Universidades e Investigación del Ministerio de Educación y Ciencia (Spain) for its financial support.

#### REFERENCES

1. K. Tennakone, V. P. S. Perera, I. R. M. Kottegoda and G. R. R. A. Kumara, "Dye-Sensitized Solid State Photovoltaic Cell Based on Composite Zinc Oxide/Tin (IV) Oxide Films", *J. Phys. D: Appl. Phys.* 32 [4] 374-379 (1999).
2. J. H. Yu and G. M. Choi, "Current-Voltage Characteristics and Selective CO Detection of Zn<sub>2</sub>SnO<sub>4</sub> and ZnO/Zn<sub>2</sub>SnO<sub>4</sub>/SnO<sub>2</sub>/Zn<sub>2</sub>SnO<sub>4</sub> Layered-Type Sensors", *Sensor Actuat. B-Chem.*, 72 [2] 141-148 (2001).

3. H. Q. Chiang, J. F. Wager, R. L. Hoffman, J. Jeong and D. A. Keszler, "High Mobility Transparent Thin-Films Transistors with Amorphous Zinc Tin Oxide Channel Layer", *Appl. Phys. Lett.*, 86 [1] Art. n° 013503 (2005).
4. Y. S. Shen and T. Zhang, "Preparation, Structure and Gas-Sensing Properties of Ultramicroc ZnSnO<sub>3</sub> Powder", *Sensor Actuat. B-Chem.*, 12 [1] 5-9 (1993).
5. D. Kovacheva and K. Petrov, "Preparation of Crystalline ZnSnO<sub>3</sub> from Li<sub>2</sub>SnO<sub>3</sub> by Low-Temperature Ion Exchange", *Solid State Ionics*, 109 [3-4] 327-332 (1998).
6. Cun W., Wang X. M., Zhao J. C., Mai B. X., Sheng G. Y., Peng P. A. and Fu J. M. "Synthesis, Characterization and Photocatalytic Property of Nano-sized Zn<sub>2</sub>SnO<sub>4</sub>", *J. Mater. Sci.*, 37 [14] 2989-2996 (2002).
7. S. Bernik and N. Daneu, "Characteristics of SnO<sub>2</sub>-doped ZnO-based Varistor Ceramics", *J. Eur. Ceram. Soc.*, 21 [10-11] 1879-1882 (2001).
8. M. A. De la Rubia, M. Peiteado, J. F. Fernández and A. C. Caballero, "Compact Shape as a Relevant Parameter for Sintering ZnO-Bi<sub>2</sub>O<sub>3</sub> Based Varistors", *J. Eur. Ceram. Soc.*, 24 [6] 1541-1544 (2004).
9. M. Peiteado, "Zinc Oxide-based ceramic varistors", *Bol. Soc. Esp. Ceram. V.* 44 [2] 77-87 (2005).
10. D. Fernández-Hevia, M. Peiteado, J. De Frutos, A. C. Caballero and J. F. Fernández, "Wide Range Dielectric Spectroscopy of ZnO-based Varistors as a Function of Sintering Time", *J. Eur. Ceram. Soc.*, 24 [6] 1205-1208 (2004).
11. D. Fernández-Hevia, A. C. Caballero, J. De Frutos and J. F. Fernández, "Application of Broadband Admittance Spectroscopy to Microstructure Control of the Electrical Properties of Ceramic Varistors", *Bol. Soc. Esp. Ceram. V.* 43 [3] 674-678 (2004).
12. A. Anastasiou, M. H. J. Lee, C. Leach and R. Freer, "Ceramic Varistors Based on ZnO-SnO<sub>2</sub>", *J. Eur. Ceram. Soc.*, 24 [6] 1171-1175 (2004).

13. M. A. De la Rubia, M. Peiteado, J. F. Fernández and A. C. Caballero, "Study at the Bi<sub>2</sub>O<sub>3</sub>-rich Region of the ZnO-Bi<sub>2</sub>O<sub>3</sub> System", *Bol. Soc. Esp. Ceram. V.* 43, 4, 745-747 (2004).
14. H. Avila, A. M. Cruz, M. Villegas, A. C. Caballero and J. E. Rodríguez-Páez, "Comparative Study of Two Synthesis Methods to Obtain ZnO-Pr<sub>2</sub>O<sub>3</sub>-CoO Ceramic Powders", *Bol. Soc. Esp. Ceram. V.*, 43, 4, 740-744 (2004).
15. D. P. Norton, S. J. Pearton, A. F. Hebard, N. Theodoropoulou, L. A. Boatner and R. G. Wilson. "Ferromagnetism in Mn-implanted ZnO:Sn Single Crystals", *Appl. Phys. Lett.*, 82 [2] 239-241 (2003).
16. J. L. Costa-Krämer, F. Briones, J. F. Fernández, A. C. Caballero, M. Villegas, M. Díaz, M. A. García and A. Hernando, "Nanostructure and Magnetic Properties of the MnZnO System, a Room Temperature Magnetic Semiconductor?", *Nanotechnology*, 16 [2] 214-218 (2005).
17. M. A. García, M. L. Ruiz-González, A. Quesada, J. L. Costa-Krämer, J. F. Fernández, S. J. Khatib, A. Wennberg, A. C. Caballero, M. S. Martín-González, M. Villegas, F. Briones, J. M. González-Calbet and A. Hernando, "Interface Double-Exchange Ferromagnetism in the Mn-Zn-O System: New Class Of Biphasic Magnetism", *Phys. Rev. Lett.*, 94 [21] 217206 1-4 (2005).
18. M. Peiteado, J. F. Fernández and A. C. Caballero, "Incorporation of Zn<sub>3</sub>Sb<sub>2</sub>O<sub>12</sub> Spinel Phase Previously Synthesized on ZnO Ceramic Varistors", *Bol. Soc. Esp. Ceram. V.*, 41, 1, 92-97 (2002).
19. M. Peiteado, J. F. Fernández and A. C. Caballero, "Processing Strategies to Control Grain Growth in ZnO Based Varistors", *J. Eur. Ceram. Soc.*, 25 [12] 2999-3003 (2005).

Recibido: 15.07.05

Aceptado: 08.02.06

